ADVANCED OPTICAL MATERIALS

Supporting Information

Effect of Mirror Quality on Optical Response of Nanoparticle-on-Mirror Plasmonic Nanocavities

Zhenxin Wang, Lufang Liu, Di Zhang, Alexey V. Krasavin, Junsheng Zheng, Chenxinyu Pan, Enxing He, Zifan Wang, Shengchengao Zhong, Zhiyong Li, Mengxin Ren, Xin Guo, Anatoly V. Zayats, Limin Tong, and Pan Wang*

Supporting Information

Effect of Mirror Quality on Optical Response of Nanoparticle-on-Mirror Plasmonic Nanocavities

Zhenxin Wang, Lufang Liu, Di Zhang, Alexey V. Krasavin, Junsheng Zheng, Chenxinyu Pan, Enxing He, Zifan Wang, Shengchengao Zhong, Zhiyong Li, Mengxin Ren, Xin Guo, Anatoly V. Zayats, Limin Tong, and Pan Wang [*]

1. SEM images of different types of gold films
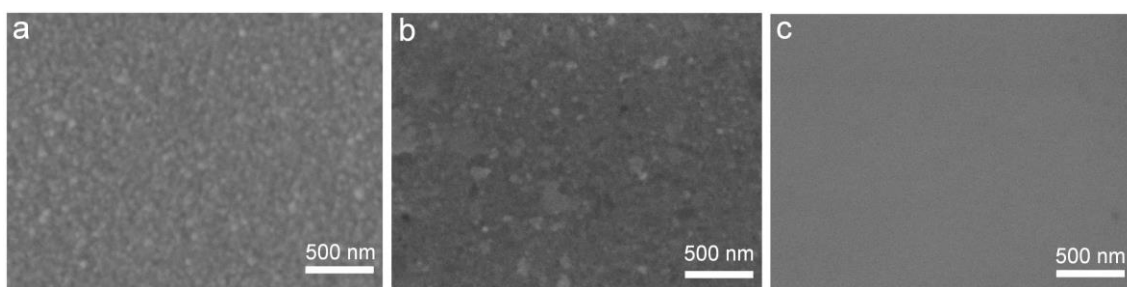
Figure S1. Representative SEM images of a) SGF, b) TSGF and c) GMF samples.

2. Measurement of different dielectric functions of different types of gold films

Figure S2a shows a schematic illustration of an experimental setup for measuring dielectric functions of gold films with an imaging ellipsometer. Figure S2b presents the measured data in the visible and near-infrared regions compared with the corresponding results from Olmon *et al.*[1] and Johnson and Christy[2]. It is worth noting that there is an obvious difference in the values of ε_1 and ε_2 for the single crystalline samples measured by Olmon *et al.* and us. In detail, the value of $|\varepsilon_1|$ for the GMF is much larger than that of the single crystalline sample studied by Olmon *et al.*, and the value of ε_2 for the GMF in the long wavelength region above 700 nm is much smaller. This is mainly due to the perfect structural quality of the chemically-grown GMFs, while for the single crystalline sample studied by Olmon *et al.*, there are lots of grooves in the film and its surface is rough.

1
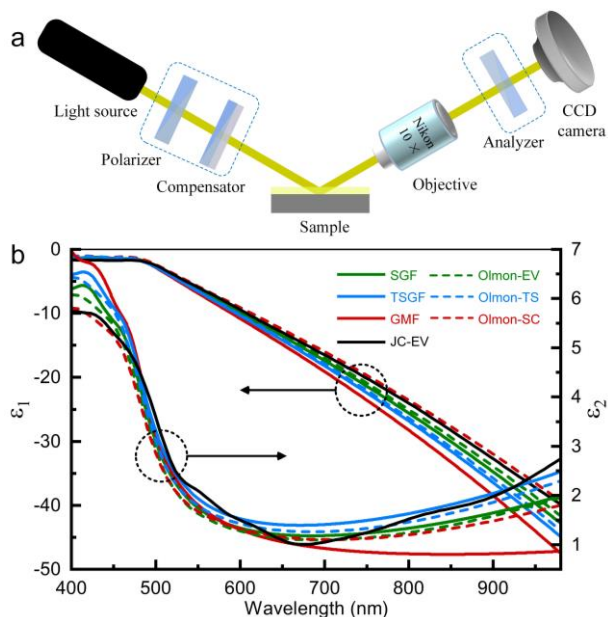
Figure S2. a) Schematic of the experimental setup utilizing a NanoFilm ep4 imaging ellipsometer. b) Dielectric function of gold in the visible spectral region for the SGF, TSGF and GMF samples compared with the data from Olmon *et al.* and Johnson and Christy (EV: evaporated, TS: template-stripped, SC: single crystal).

3. TEM images of gold nanospheres and silver nanocubes
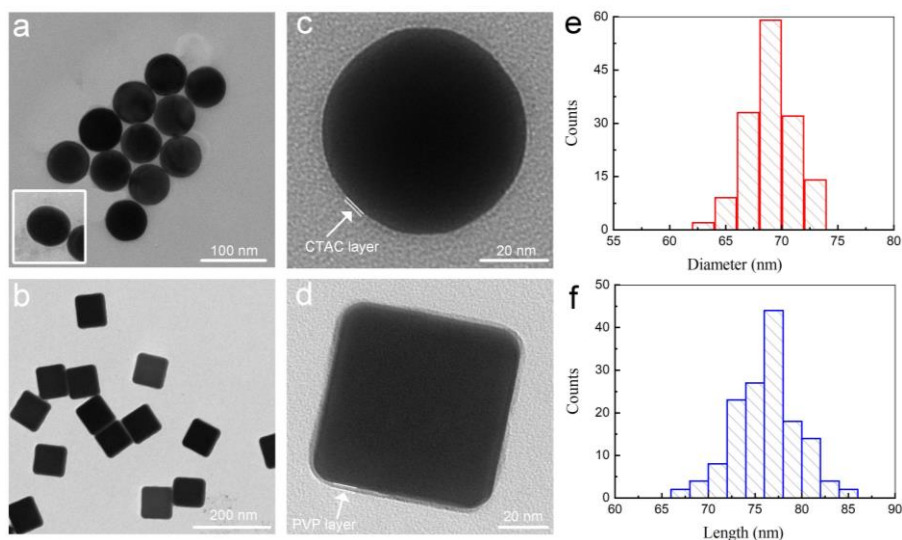
Figure S3. a-d) TEM images of (a,c) nanospheres and (b,d) nanocubes. The RMS roughness of the gold nanospheres and silver nanocubes is estimated to be at the same level of ~0.3 nm based on the enlarged TEM images. e,f) Size distributions of (e) gold nanospheres and (f) silver nanocubes.".

4. Dark-field spectroscopy setup

Scattering from single nanocavities was studied via dark-field scattering spectroscopy, as schematically shown in Figure S4a. Briefly, unpolarized white light from a tungsten-halogen lamp was first focused onto nanocavities at an incident angle of 68° by a 100× dark-field objective (NA = 0.8, TU Plan ELWD, Nikon). The scattered light from the nanocavities was collected by the same objective and directed into a charge-coupled device (CCD) camera (DS-Fi3, Nikon) for real-time imaging and a spectrometer (QE pro, Ocean Insight) for a spectral analysis. All the scattering spectra were measured under the same illuminating condition (as well as surrounding temperature and humidity) and using the same integration time. The nanocavities were randomly selected and only those separated from their nearest neighbor by at least several micrometers were chosen to ensure thescattering measurements at a single nanostructure level. The measured scattering spectra were calibrated by the spectrum of the used white lamp and the spectral response of the detection system (Figure S4b).
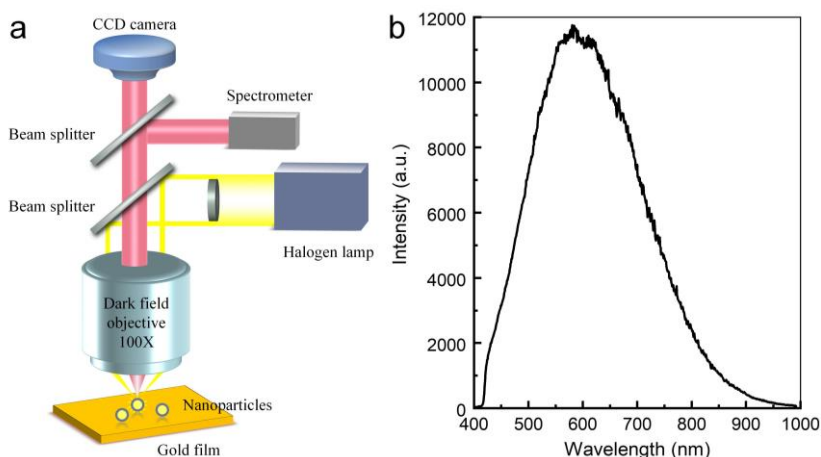
Figure S4. a) Schematic diagram of the dark-field scattering spectroscopy setup. b) Measured spectrum of the white light source of the dark-field spectroscopy setup, collected by the detection system, providing a complete data set for the normalization of the results.

5. Dark-field scattering spectra and table list of corresponding statistical data of NSoM nanocavities
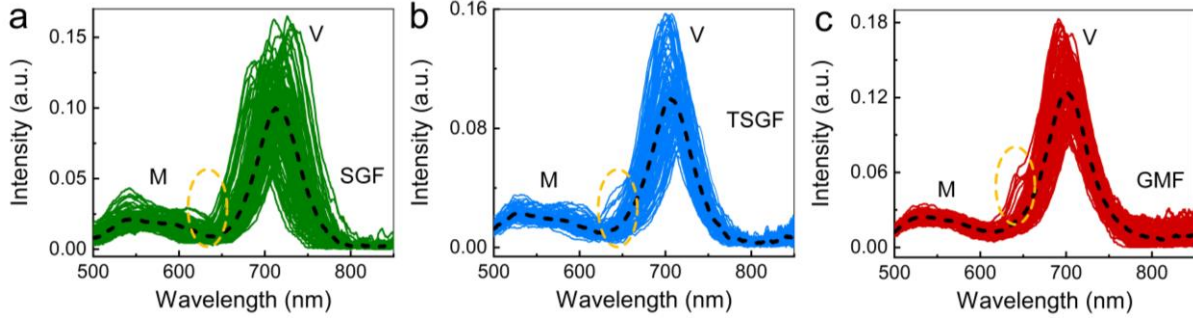
Figure S5. a-c) Superimposed dark-field scattering spectra of 100 NSoM nanocavities formed on the (a) SGF, (b) TSGF, (c) GMF. Orange dashed circles indicate the newly emerged mode for nanocavities formed on TSGF and GMF.

Table S1. Summary of 100 groups of statistical data for NSoM nanocavities

Sample	NSoM nanocavity (mode V)		
	Average peak position (nm)	Average Quality factor	Average peak intensity (a.u.)
SGF	712.2 ± 11.9	12.52 ± 1.4	0.09
TSGF	702.9 ± 7.9	13.06 ± 1.2	0.09
GMF	699.2 ± 7.2	13.95 ± 1.2	0.12

6. Dark-field scattering spectra and table list of corresponding statistical data of NCoM nanocavities
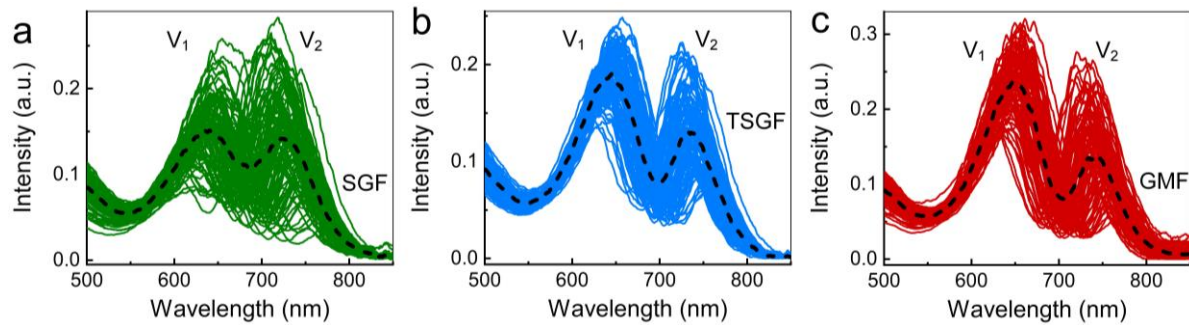
Figure S6. a-c) Superimposed dark-field scattering spectra of 100 NCoM nanocavities formed on the (a) SGF, (b) TSGF, (c) GMF.

Table S2. Summary of 100 groups of statistical data for NCoM nanocavities

Sample	NCoM nanocavity					
	Mode V_1			Mode V_2		
	Average peak position (nm)	Average Quality factor	Average peak intensity (a.u.)	Average peak position (nm)	Average Quality factor	Average peak intensity (a.u.)
SGF	645.5 ± 15.5	9.9 ± 2.1	0.13	735.1 ± 13.5	12.7 ± 3.5	0.16
TSGF	653.8 ± 8.9	9.2 ± 1.0	0.13	741.7 ± 8.5	14.6 ± 3.5	0.13
GMF	657.6 ± 9.1	9.5 ± 1.0	0.23	744.1 ± 9.8	18.8 ± 4.1	0.15

7. Quality factor calculation of the plasmon resonance modes

The quality factors of various resonance modes were calculated as follows. The scattering spectra were firstly transformed into the frequency domain. Then, the data were fitted with sums of two or three Lorentzian terms for NSoM nanocavities (Figure S7a,b for two or three peaks fitting) or Fano line shapes[3] (reflecting the hybridization of the modes) for NCoM nanocavities (Figure S7c). The red lines represent the obtained fitting curve, which show good agreement with original data (black dash lines). After that, the central frequency (ω) and full-width at half-maximums (FWHM) of each peak were taken from the fitted parameters. Finally, the quality factors were calculated as the ratios of ω to FWHM.
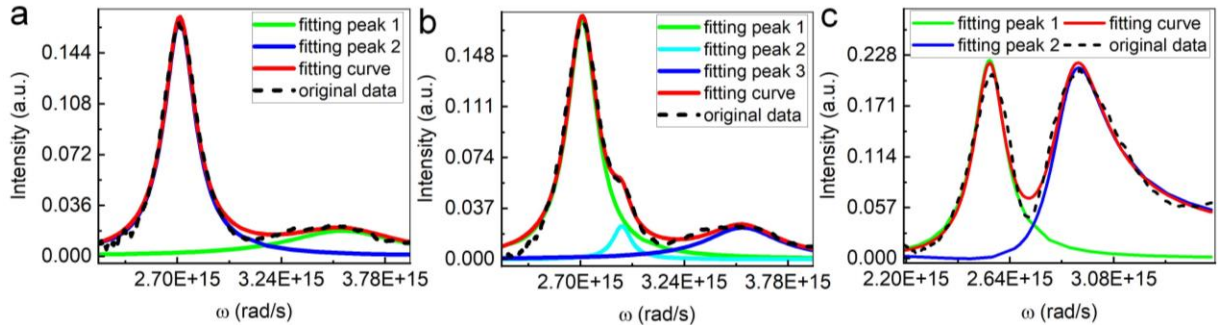
Figure S7. Fits of the frequency-domain scattering spectra. a,b) Two- (a) or three- (b) term Lorentz fits of the measured scattering spectra from the NSoM nanocavities. c) Fit of the measured scattering spectrum from the NCoM nanocavities with Fano line shapes.

8. Structural parameters for nanocavities
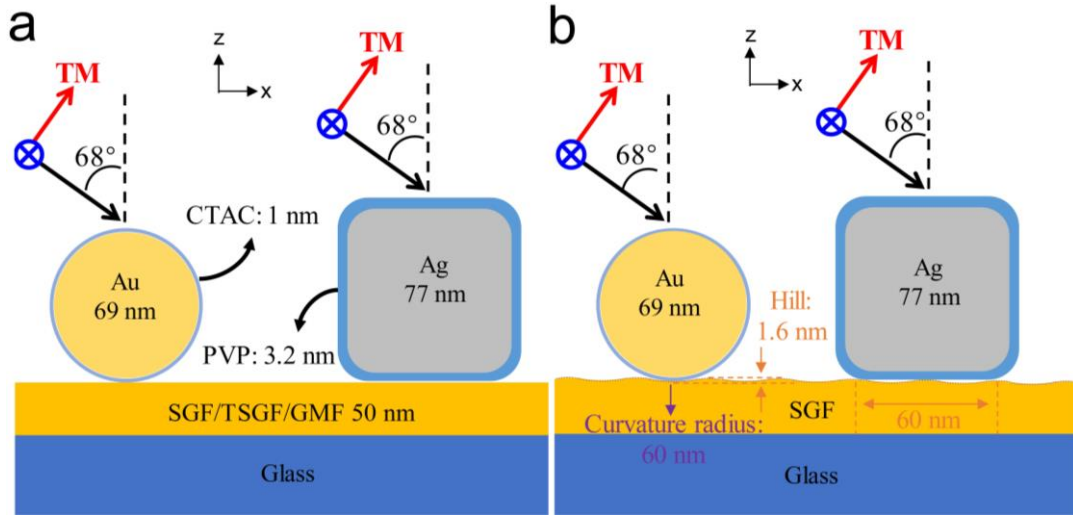
Figure S8. Structural parameters of the NPoM nanocavities used in the simulations for (a) gold films with an ideally smooth surface, (b) gold films with a rough surface.

9. Detail on the optical constant fitting with a superimposed line shape

The spectra of Ψ and Δ were fitted by the appendent data processing software of the ellipsometer to obtain the values of n and k. A superimposed line shape (Drude + three-Lorentz) was used in the fits to extract the effective n and k. The expression of the Drude model is written as $\varepsilon(E) = eps - \frac{A}{E^2 + i\Gamma E}$. The item '$eps$' denotes $\varepsilon(\infty)$, which is an additional fitting parameter and has no correlation with other parameters.[4] The expression of Lorentz oscillator model is written as $\varepsilon(E) = \frac{AE_0}{E_0{}^2 - E^2 - i\Gamma E}$, where E_0 is the resonance energy and AE_0 is the oscillator strength, Γ is the

damping constant. To evaluate the goodness of the fitting, root mean square error (*RMSE*) is defined by

$$RMSE = \sqrt{\frac{1}{N-P+1}\chi^2}$$

Where *P* stands for the number of fit parameters, $\chi^2 = \sum_{n=1}^{N} \frac{(Y_{n,data}-Y_{n,model})^2}{\sigma_n^2}$, N is the number of experimental data, $Y_{n,data}$ is the experimental data, $Y_{n,model}$ is the modeled data, σ_n is the standard deviation of data Y_n. The *RMSE* should be close to one for an ideal fit. We keep on changing the fitting parameters until the optimal RMSE were obtained. The parameters used in the fitting are provided in Table S3.

Table S3. Fitting parameters of the optical constants

Sample	Lorentz 1			Lorentz 2			Lorentz 3			eps	Drude		RMSE
	E_0	AE_0	Γ	E_0	AE_0	Γ	E_0	AE_0	Γ		A	Γ	
GMF	2.63	0.97	0.26	2.86	4.19	0.53	3.43	24.46	1.00	6.10	90.91	0.01	4.36
TSGF	2.66	1.82	0.37	2.95	6.69	0.63	3.55	20.55	0.75	5.29	85.46	0.05	2.82
SGF	2.67	2.05	0.39	2.97	6.68	0.63	3.57	19.04	0.68	4.93	81.31	0.04	1.96

References

[1]   R. L. Olmon, B. Slovick, T. W. Johnson, D. Shelton, S.-H. Oh, G. D. Boreman, M. B. Raschke, *Phys. Rev. B* **2012**, *86*, 235147.

[2]   P. B. Johnson, R. W. Christy, *Phys. Rev. B* **1972**, *6*, 4370.

[3]   S. Zhang, K. Bao, N. J. Halas, H. Xu, P. Nordlander, *Nano Lett.* **2011**, *11*, 1657.

[4]   G. E. J. Jr., F. A. Modine, *Appl. Phys. Lett.* **1996**, *69*, 371.